CONC-760312 3-1

CORROSION OF VALVE METALS

by

J. E. Draley

Prepared for

American Chemical Society Symposium

Chicago, IL

March 30, 1976

UofC-AUA-USDOE

ARGONNE NATIONAL LABORATORY, ARGONNE, ILLINOIS

Prepared for the U. S. DEPARTMENT OF ENERGY
under Contract W-31-109-Eng-38

CORROSION OF VALVE METALS*

by

J. E. Draley

Argonne National Laboratory

I had a little problem deciding what kind of talk to give you. I concluded that it should not be a general survey of everything I can find that is related to corrosion of valve metals or film-forming metals; that it should not contain just one or two topics within that subject--about which I could talk enough to give you some depth--but a compromise between these two. Secondly, I had to decide whether to talk theoretically or mathematically, on the one hand, or phenomenologically on the other, and I have chosen the latter approach. My intent is to give you some perspective about the way these materials corrode. I have selected some examples that I think are sufficiently general and illustrate the principles well enough to do this. Many of the slides are taken from our own work of some years ago. It must be acknowledged that the unique corrosion characteristics of a number of the valve metals are not identified, and behavior in a number of common environments is not addressed.

First of all, I have found the title valve metals to be confusing for a number of people; for example, someone asked if they are the metals of which valves are made. Let me give you a few guidelines. First, the valve metals form relatively perfect oxide films. That means they are relatively perfect with respect to protection against corrosion, which we shall amplify a little. Secondly, they are relatively perfect insofar as there is not much local breakdown or leakage when they are anodized. Partly related to that there are high fields in these oxides during the period of growth--fields greater than about 10^6 volts/cm.

In the first figure, we see illustrated a relationship often drawn between the energy of the bond between oxygen and the metal and the field required to produce an anodic film. In this instance, the field is that

---

*Presented as a lecture on the Chemistry of Corrosion sponsored by the Chicago Section of the American Chemical Society in conjunction with the Chicago Section of the Electrochemical Society and the National Association of Corrosion Engineers, March 30, 1976.

which corresponds to a given small current in anodizing, or production of the oxide film. The factors responsible for sound and protective films are not well known. It is still a bit of a mystery why some systems form better films than others. A number of individual principles have been brought up. Pilling and Bedworth years ago wrote that if the volume of the oxide produced on a metal surface is less than the volume of metal from which it is produced, there is little chance that the oxide film will be protective. As stated, that is a good guiding principle, but of all the systems for which there is expansion in the formation of oxide, the rule doesn't predict reliably which oxides will be protective and which will not.

Strong bonding between the oxide and the metal substrate seems to be essential to the formation of highly protective films. That's one principle I think you can hold on to. The others don't work very wel' There are a lot of peculiarities; for example, in some cases the oxygen dissolves significantly in the surface layers of the metal. This doubtless reduces the effective size of the surface metal atoms and allows adjustment of the positions of the surface atoms of the substrate so they will nearly match the positions of the contiguous cations in the oxides.

Figure 2 shows that which metals form good films depends not only on the bond energy but also on the solution in which the films are formed. These curves are for anodizing aluminum in a series of solutions. The top 5 curves are for a family of solutions in which the films remain resistant to greater thicknesses than for the two less ideal solutions. In other solutions, one can't get anodized films at all. The resistivity on the ordinate is for the film itself. I think it is important to note that many metals form hydrated oxides, in which hydroxide ions are constituents. As a general rule, highly protective films are anhydrous; it is often speculated that the high field present during the formation of the film (vide supra) contributes to the formation of anhydrous rather than the hydrated oxide. It is easy to see that a high field operates when one anodizes by the application of a potential; it is less obvious, but evidently equally true during unassisted thin-film oxidation. Local fields from multiply-charged cations might contribute to the formation of compact, anhydrous oxides; the best films usually contain cations with a charge of 3 or more. One more thing about films: they often are not very stable in water or in aqueous solutions. This tends to cause confusion about the protectiveness of

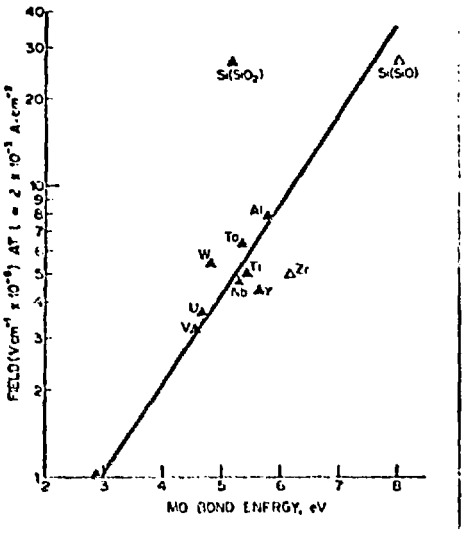

Figure 1. Field required to sustain an ionic current density of 2×10^{-3} A·cm^{-2} for anodic oxides as function of metal-oxide bond energy (1). Reprinted courtesy Electrochem. Soc.

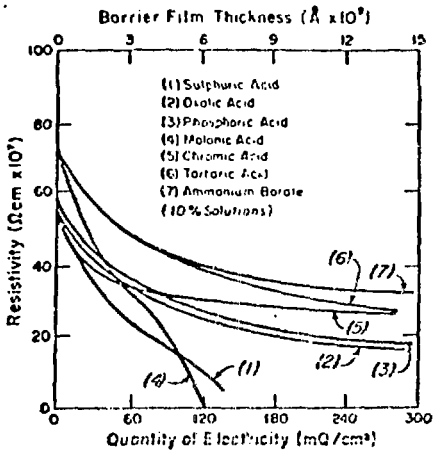

Figure 2. Differential specific resistance for growing barrier films on aluminum (2). Reprinted courtesy Pergamon Press.

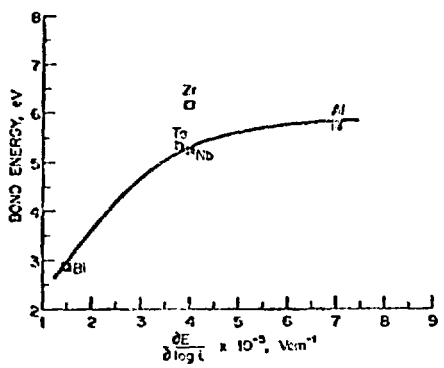

Figure 3. Relationship between metal-oxygen bond energy and Tafel slope for film growth (1). Reprinted courtesy Electrochem. Soc.

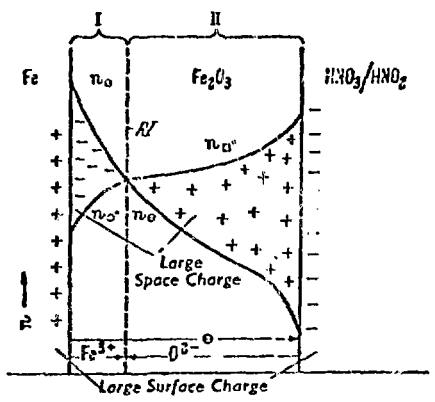

Figure 4. Schematic representation of the concentration of the free electrons and ion defect positions in the homogeneously structured passive layer Fe_2O_3 with space-charge inversion (3). Reprinted courtesy Plenum Press.

oxide films. The film itself may be a very good one, but it may deteriorate, sometimes slowly, sometimes rapidly; sometimes rather generally and sometimes locally. Its protectiveness thus may be temporary or imperfect as a function of time. One of the conundrums about such protective films has always been how to rationalize the demonstrated requirement to adsorb species on some metal surfaces or on some metal oxide surfaces to provide protection. It appears to me that the function of the adsorbate is to protect the oxide film against the hydrating or solvating effect of the water. The film itself is good enough, then, to provide protection.

In Figure 3 we see the relationship between metal-oxide bond energy and the Tafel slope--the relationship between potential and log current during oxide film formation. It says, in effect that when the bond energy is higher, it takes more voltage increase for a given increase in current, which is to say that when the bond energy is higher it is more difficult to pass extra current through a more protective film.

Corrosion and oxidation of valve metals generally consist both of the growth and degradation of oxide films. I'd like to begin discussion of the growth of oxide films with Figure 4, taken from Hauffe(3). In this case iron is oxidized directly to ferric oxide in a nitric-nitrous acid solution. The author has suggested the existence of concentration gradients for cation lattice defects, oxygen vacancies, and electrons. During the growth of the film, it is proposed that electrons, cations, and anions migrate. A large space charge variation is proposed within the oxide film--a case which was ignored for years by people who studied oxidation. The resultant combination of fields from surface charges and from the space charge leads to no electrical field at the interface between Zones I and II at which location new oxide is proposed to form. Other more complicated models have been developed; I have chosen to show this because of its generally applicable principles.

In Figure 5 we see that sometimes seemingly perfect thin films are far from perfect. This is for an aluminum alloy that, from some techniques, would appear to carry a perfect film. You see some of a series of platelets growing out in this transmission electron micrograph taken across an edge. Figure 6 shows a case in which oxide nuclei grow on a metal surface. This one is for iron in low pressure oxygen; similar results have been observed for other metals. If one looks at this surface during oxidation, one sees only a very thin

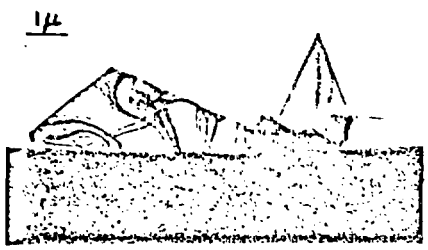

Figure 5. Oxide platelets viewed by electron silhouette on aluminum after corrosion for 30 hours in steam at 540°C (4). Reprinted courtesy Academic Press.

Figure 6. Oxide nuclei on (111) iron foil after oxidation at 540°C and 1.1×10^{-5} torr for 55 minutes (5). Reprinted courtesy Maruzen Co., Ltd.

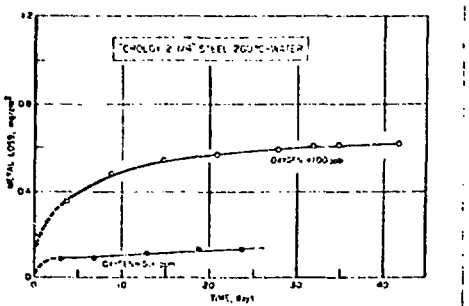

Figure 7. Corrosion of Croloy 2¼ steel in water at 260°C (6). Reproduced courtesy National Assoc. Corrosion Engineers.

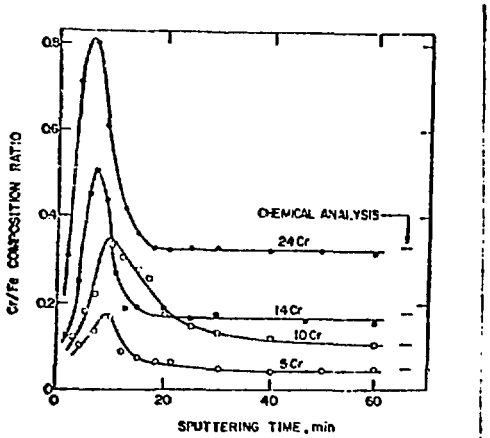

Figure 8. Cr/Fe ratio as a function of distance from surface for four oxidized iron-chromium alloys (7). Ratios for alloys on right. Reprinted courtesy Electrochem. Soc.

film until nuclei show up at the same time at many places over the surface. These crystals then grow at measurable rates. Their orientation can be determined and related to the orientation of the metal substrate.

I'd now like to show you some unpublished color photographs of a series of iron samples which were oxidized for three days in water at elevated temperatures. We've changed the potential for oxidation by using different concentrations of oxygen in water. With 290 ppm oxygen concentration at 260°C, a highly perfect ferric oxide film formed showing a little tint of interference color--that is often valuable for giving some clues. The color indicates that the thickness is uniform over a big enough area to develop the interference color; in a few minutes, we'll see that thicknesses sometimes vary from grain to grain. At 35 ppm oxygen areas of breakdown are observed. The next slide shows some photographs of samples at 150°C, but otherwise at the same conditions. You'll see that for the same oxygen concentrations in the water the protection is not as good. A greater oxidizing potential (oxygen concentration) is required for a highly protective film as the temperature is lowered; the trend continues to at least as low as 100°C (third slide) at which temperature 540 ppm O_2 provided an excellent film(6). To the best of my knowledge, nobody has used this system to maintain the potentially excellent aqueous corrosion resistance of iron. The next slide shows a range of interference colors for contiguous grains on a specimen of iron, under conditions identical to those shown earlier. If there is a deficiency of oxygen--insufficient oxygen to provide good protection--sizeable pits are formed in pure water. A lesson from this is that pitting doesn't occur only in strong electrolytes or selected electrolyte solutions.

If the composition of the alloy is changed the composition of the oxide changes, and it is possible to make the oxide considerably more protective on a metal like iron. The next slide shows the effect of a little bit of chromium. Croloy-5 contains 5% chromium and some molybdenum; you can see that at 260°C with 35 ppm O_2 corrosion resistance is substantially better than that of iron. As shown in Figure 7 the corrosion behavior of such alloys also seems favorably influenced by high oxygen concentration in water. In Figure 8 it is seen that there is considerable chromium enrichment in the oxide films on oxidized iron-chromium alloys; evidently the greater protectiveness of the films for the chromium-bearing alloys is related to this composition. Figure 9 shows that the ratio of oxygen to

metal also varies within the film. That corresponding to M_2O_3 is shown. As one gets closer to the metal, shown by surface analysis after sputtering some material off the surface, the oxide is seen to have less oxygen in it. It is another peculiarity of some of these systems that in the thin film range, the stoichiometry of the oxide is not as expected.

As most of you know, if nickel is added to chromium alloys a series of stainless steels is produced with quite good corrosion resistance. These alloys have a widespread use; these days those with compositions close to 18 Cr-8 Ni are increasingly being used in many practical applications. I guess I should warn you that if you listened to Roger Staehle you heard that there are a number of instances when they also crack unexpectedly after a period of exposure. So they are by no means perfectly resistant to corrosion; nevertheless, they offer a very substantial improvement in the performance of low to moderate cost materials. Figure 10 is made up to show that if aluminum is added to 304 stainless steel--that is roughly the simple 18 and 8 stainless steel--the corrosion protection provided by the oxide to superheated steam is very markedly increased. This element also increases resistance to oxidation by gases--air, oxygen, and carbon dioxide. Aluminum is an effective alloying constituent for improving the corrosion-oxidation resistance of iron as well. The protective film is enriched in aluminum as compared to the metal composition. In both systems, the alloys containing aluminum tend to be brittle.

I have been talking to you about the formation of oxide films; for completeness it is appropriate to mention that films also grow or form by recrystallization of a substrate layer or by hydration of a material that was originally formed in an anhydrous form. As a general rule, those cases produce films that are not highly protective. There is a practical exception to that: if one anodizes aluminum in some environments, notably sulfuric acid, the coating is relatively porous, with the oxide only partially hydrated. By boiling in water, hydration is increased, the volume of the oxide is increased and the pores are sealed, and an effective protective layer is formed.

I'd like to switch now and talk to you about degradation of films. In order to talk about corrosion one has to consider both the growth of films and their degradation. As one studies them, one finds that the combination of the two is the key to getting a measure of understanding of the behavior of the system. Some of the results are a little unexpected at first glance.

It is well for us to be alert for such things. Let me make an obvious platitude for you about a film that degrades at a constant rate. It is obvious that the metal will corrode at a constant rate if degradation is uniform all over the surface, although it might take some time to reach that stage while it builds up a film. That is not a rare phenomenon. It is more common, I think for degradation not to be that uniform over the surface. We're going to talk about some of those cases.

First, let us consider a rather simple case: the film dissolves in water. When iron or steel corrodes in high temperature water without oxygen, the rate of corrosion is determined by the rate at which the film dissolves and is lost from the surface. This rate remains constant if there is some procedure that cleans up the water and keeps it from becoming saturated. One such procedure is passage through a loop containing a lower temperature septum in which some of the material precipitates. Another is passage through an ion exchange resin or some other device that will purify the water. Such loop systems often contain suspended solid corrosion product in the water. This material in nuclear reactor systems is called crud and it has been the source of a lot of irritation and money. These come about because the crud is radioactive and deposits in all parts of the system, complicating maintenance.

If one chooses the temperature and the alloy (e.g. A288 containing 1% Ni) aluminum forms in water a film such that the rate of formation is inversely proportional to the thickness. That gives what's called the parabolic growth law; data for such behavior are shown in Figure 11 (together with a dashed curve for another experiment). In the kind of system in which fresh water is continuously added and the excess allowed simply to leak out, at least a partially saturated solution is lost all of the time. The two specimens of Figure 12 have been fitted by curves that have the same growth rate constant as in Figure 11 and different dissolution rates. They were in the same autoclave at slightly different locations; probably the water contained a little more dissolved aluminum at one specimen than at the other. The expression for the paralinear behavior in its simple form is:

$$\frac{dL}{dt} = \frac{k_p}{L-(g+ft)} \quad ,$$

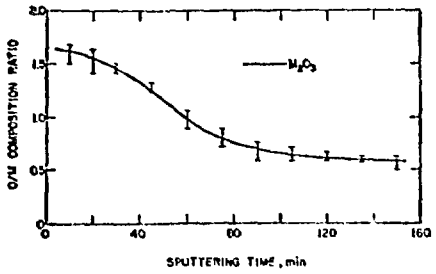

Figure 9. O/M ratio as a function of depth in oxide in iron and iron-chromium alloys (7). Reprinted courtesy Electrochem. Soc.

% Al	Metal Loss, mg/cm²
0	18.0
1	17.0
2	8.8
4	0.06
5	0.03

Samples exposed in as cast condition, surfaces electropolished.

Figure 10. Corrosion of aluminum-modified Type 304 SS for 28 days in steam contg. 30 ppm O_2 at 650°C (8). Reprinted courtesy Nat'l. Assoc. Corrosion Engineers.

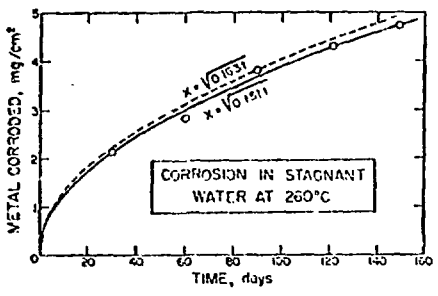

Figure 11. Parabolic corrosion of experimental aluminum alloy A288 (Al+1%Ni, 0.5%Fe, 0.1%Ti) in unrefreshed water (9).

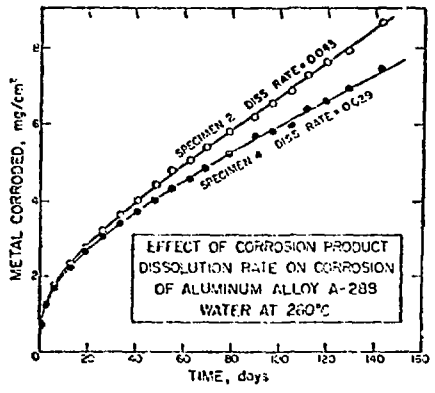

Figure 12. Paralinear corrosion of aluminum alloy A288 in refreshed water (9).

where L is the amount of metal loss (determined through the use of a special metal thickness gauge), k_p the parabolic growth constant, f the rate of dissolution for the specimen, and g the amount of dissolution that occurs early in the exposure. At long times the curve for L versus time resembles a straight line with slope f.

Paralinear corrosion (related to dissolution of corrosion product) does not occur for all aluminum alloys in water at all high temperatures. In Figure 13 are plotted data for an alloy (Al, 1% Ni, 0.1% Ti) corroded in water at 350°C (10). The corrosion rate was low and constant, as shown better in other figures in the same publication. For some specimens in the figure 1/3 or 2/3 of the corrosion product was removed mechanically after the first exposure period. There was no discernible effect on subsequent corrosion, indicating that control of corrosion probably resided close to the metal-oxide interface. Similar experiments for the alloys and temperatures where paralinear behavior occurs showed that removing some of the product caused an increase in subsequent corrosion rate.

The use of Figure 14 begins discussion about low temperature corrosion of aluminum in water. Again we'll see that the total film is not controlling. This is the kind of curve obtained in a couple of tests that ran for a long time in continuously refreshed systems. Note that the rate is decreasing continually with time for at least a few years--we'll analyze that curve shape starting with Figure 15. At the beginning of the tests (from 0.1 to nearly 10 hours) and subsequent to about 100 hours, the weight gain and the metal corroded (determined through the use of a sensitive metal thickness gauge) varied as the logarithm of time. The initial film is boehmite, the same partly hydrated oxide that forms at high temperatures. When this film breaks down, beginning in half a day at these conditions, we find that the total amount of corrosion and the total oxide present quickly increase severalfold. The new product is the completely hydrated oxide bayerite. If one runs the test a long time (Figure 16) one finds that the logarithmic rate law holds. The dashed lines indicate that the initial period is sensitive to the test procedure that is used. The height of the plateau varies inversely with how well refreshed the solution is. The requirement for measurement sensitivity in this test was substantial. As a matter of fact, the (eddy current) gauge limitation came not by its sensitivity (about ten Angstrom units in diameter for

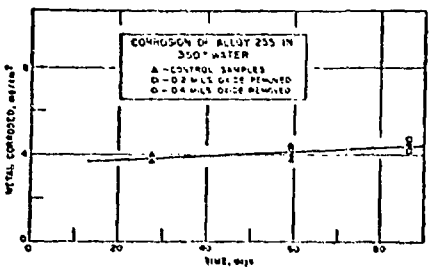

Figure 13. Influence of corrosion oxide removal on the corrosion of an Al-1Ni-0.1Ti alloy (10). Reprinted courtesy North-Holland Publishing Co.

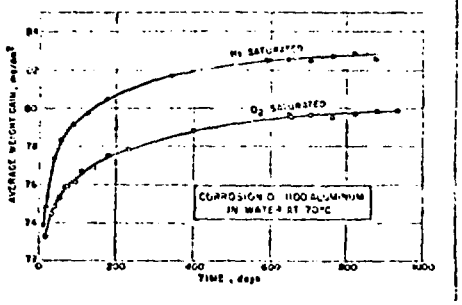

Figure 14. Corrosion experiments in water at two oxygen concentrations (<0.4 and 19 mg/ℓ) (11).

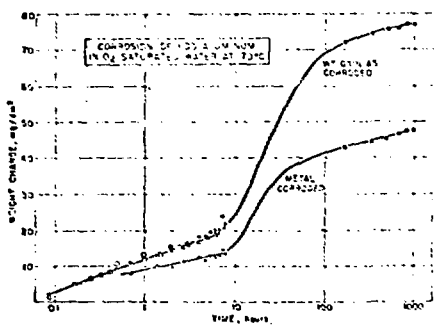

Figure 15. Early stages in corrosion of aluminum (11).

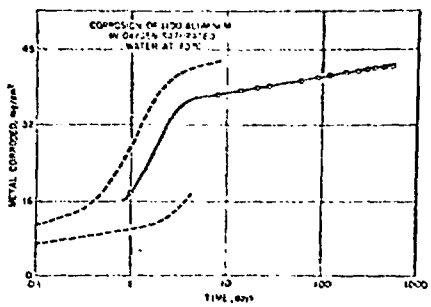

Figure 16. Long-time corrosion of aluminum (12).

a round specimen) but because of the metallurgical changes that occurred in the samples.

Now I'd like to analyze what happens to the oxide during the second logarithmic corrosion period. Figure 17 shows the amount of aluminum dissolved from a specimen (1100 aluminum) and carried away in the discharge water. This was determined by very carefully collecting the effluent solution, boiling off the water, collecting the aluminum, and analyzing the microgram quantities. Dissolution (amount = ξ) occurred at a constant rate during the second logarithmic period. Combining these data with weight gain (G) and metal lost from the single specimen (L), the amount of boehmite (a) and the amount of bayerite (b) shown in Figure 18 were calculated (13). The curve for boehmite layer growth close to the metal closely follows the curve for the amount of corrosion (both even showing an atypical increase in slope near the end), while the amount of bayerite slowly decreases (presumably by dissolution). The evidence is that in this system boehmite makes a protective (rate-controlling) layer while the bayerite dissolves and obscures the truth.

I would like to tell you about another kind of unusual kinetic behavior, that of zirconium. An alloy called Zircaloy 2 contains minor amounts of iron, chromium and nickel and a little tin. The alloy was invented by accidentally contaminating a zirconium-tin alloy with stainless steel. Since that time people have been making it on purpose. The weight-gain slopes on the log-log plot in Figure 19 are approximately 1/3 and the rate expression that is nearly followed is called cubic oxidation. It occurs initially in water; it is followed by film breakdown and an increase in oxidation rate with new kinetics (showing straight lines and slopes very close to 1 on this plot). A log-log straight line with a slope of one is unusual, since it requires the particular straight line on cartesian coordinates that passes through the origin. At the time of "breakaway" there is a recrystallization of the zirconium oxide to a less coherent film. That is an additional form of degradation.

Lest you believe things are too simple during "cubic" oxidation I've chosen to show this slide (Figure 20) based on data by Bob Shannon at Hanford, Washington, which shows that individual specimens corrode in series of waves. Paul Pemsler once christened those the Picturesque Hills of Shannon during a meeting. What this illustrates is that we're not

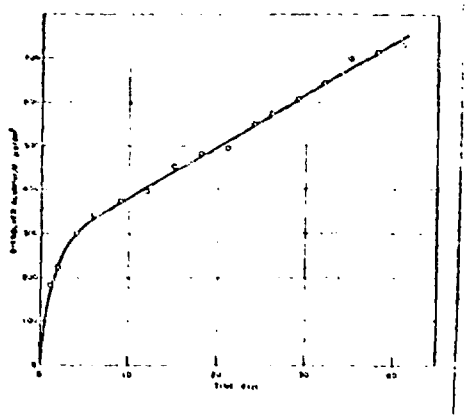

Figure 17. Corrosion product dissolved from specimen of Fig. 18 (13). Reprinted courtesy Electrochem. Soc.

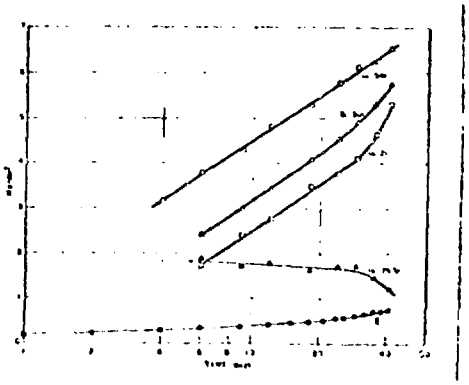

Figure 18. Summary of corrosion for one specimen of 1100 aluminum in oxygenated water at 70°C (13). Reprinted courtesy Electrochem. Soc.

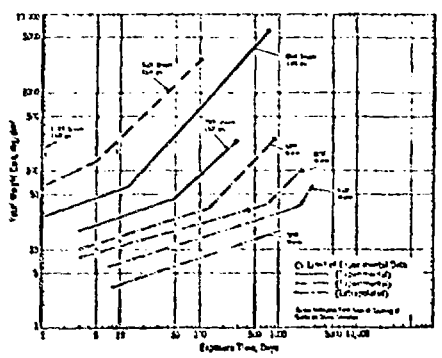

Figure 19. Corrosion of beta-quenched Zircaloy-2 in water and steam (14).

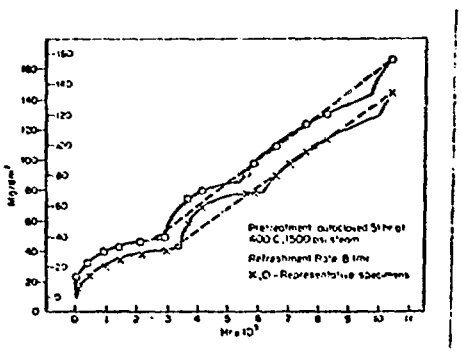

Figure 20. Corrosion weight gain of Zircaloy-2 in water at 360°C (15).

dealing with continuous films continuously growing without breakdown. It happens that the breakdown on these specimens occurred over much of the surface at the same time so the phenomenon is visible. If it occurred locally and not at the same time at different places, you would not see the "hills", but odd kinetics such as roughly cubic. The phenomenon is by no means unique to zirconium. Figure 21 shows similar behavior by aluminum, also in high temperature water.

The oxidation of zirconium in oxygen at elevated temperatures follows near-cubic kinetics for awhile, then parabolic kinetics. A number of efforts have been made to explain the near-cubic behavior, with localized or line diffusion as that perhaps generally preferred. I'll describe for you my own thinking, put together and presented informally in 1967. It has not been published. At 700°C there is an initial layer of zirconium oxide that is relatively perfect, that forms interference colors on small areas; the rate of growth of film and the rate of diffusion of oxygen into the metal depend on the orientation of the metal crystal. Polycrystalline specimens prepared metallurgically in different ways, always pure and equally carefully treated, oxidize at quite different rates initially, but the rates become equal at long (parabolic) times. To fit these facts I developed the following model. The film that grows on the metal surface is proposed to be unique and different from the one that is stable on the outside and at long times. X-ray diffraction patterns taken in our laboratory during initial oxidation (special apparatus) suggest that this oxide is tetragonal rather than the commonly found monoclinic oxide. At any small area on the surface, for example for a single crystal surface, the initial film grows and oxygen diffuses into the metal at rates that are unique for that area until the film thickness reaches the value s (proposed to be the same for all areas). The initial film then transforms nearly instantaneously into final film, and the initial film then grows again in a second cycle, again to the limiting thickness s. The parabolic rate constant for the final film is c (value the same for all areas) and the rate of growth of initial film at a particular area is

$$\frac{dx_i}{dt} = \frac{b_i}{x_i + \frac{b_i}{c}(n-1)s} - \sqrt{\frac{k_i}{2t}} \quad ,$$

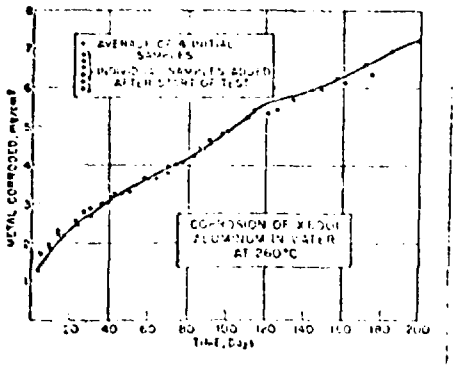

Figure 21. Corrosion of an aluminum alloy (1100 Al + 1% Ni) in high-temperature water (9).

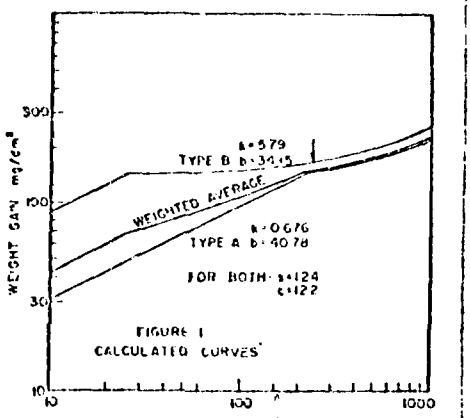

Figure 22. Calculated curves for oxidation of zirconium grains at 700°C (16).

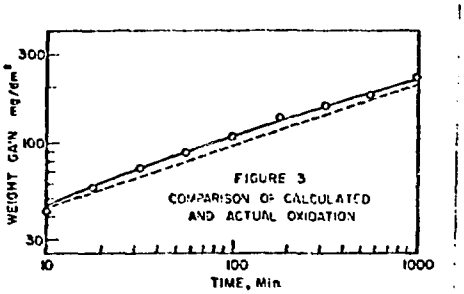

Figure 23. Oxidation of polycrystalline zirconium at 700°C (16).

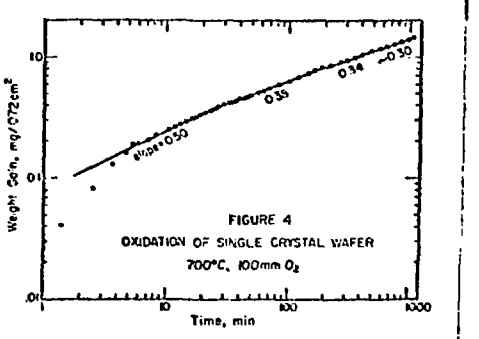

Figure 24. Observed oxidation of zirconium crystal (16).

where n is the number of the growth cycle at time t and k_i is the local diffusion constant for oxygen in metal.

An estimate of the type of oxidation curve to be expected from this model was developed from an initial case where two types of surfaces (A and B) were identified, and rate constants assigned that were not in conflict with any known data. Weight gains expected for the first thousand minutes are shown in Figure 22 for areas A and B and for a specimen consisting of 80% type A and 20% type B. The ends of the first growth cycle for each area can be identified. A number of weight-gain points for this hypothetical specimen are plotted in Figure 23 along with a reproduced weight gain recorder tracing (the solid line). A perfect cubic line is also shown for comparison (dashed line).

The fit is so good that it seems highly likely that the use of more types of areas to smooth out the average in the model would lead to excellent fitting of real-sample data. It isn't possible to say much more at this time; I do believe that the weight-gain curve for the single crystal wafer (more than 80% of area of one orientation) shown in Figure 24 displays breaks and slopes of the right order for the segments on a log-log plot. My personal conviction is that some kind of statistical models are going to be required to fit correctly much of the corrosion and oxidation data of the valve metals.

You've heard electrochemistry of corrosion as a lecture; I shouldn't spend much time on it but I'd like to describe some electrochemical effects for film formers. First the general principles. If you put a good electronic conductor (a metal) in an aqueous solution, you will typically find that an electrical potential is developed between the piece of conductor and the solution. When ions of the metal enter the solution and leave extra electrons behind a negative potential is developed. All oxidation reactions occurring on the surface are expected to produce this result. Similarly, reduction reactions that use electrons from the metal are expected to produce a more positive potential in the metal. The solution potential of the metal influences the rate of an electrochemical half-cell reaction in accordance with Le Chatelier's Principle, so it is possible to predict through the use of the Nernst Equation the potential that will exist when the only significantly rapid reactions are the oxidation and reduction parts of a reversible reaction. When more than one potentially reversible process occurs, the rate of oxidation will be expected to exceed the rate of reduction for at least one and the converse for at least one. At

a steady-state potential, the sum of the rates of all of the anodic reactions will equal the sum of the rates of all the cathodic reactions.

For film formers, a typical anodic reaction is

$$M + H_2O \rightarrow MOH + H^+ + e^- ,$$

so an oxide is formed and the solution becomes acid. The most common cathodic reactions are

$$H_2O + e^- \rightarrow 1/2\ H_2 + OH^- \quad \text{and}$$

$$1/2\ O_2 + 2H_2O + 2e^- \rightarrow 2OH^- ,$$

so cathodic reactions produce alkali. Directly related to the pH are the stabilities of the various species for the corroding metal. Thus for iron, the so-called Pourbaix Diagram for iron in Figure 25 shows potential-pH zones in which Fe_2O_3 or $Fe(OH)_2$ are stable and thus in which protective films of these substances might form at a total ionic concentration of 10^{-6} M.

When a film is present, the hydrogen produced from the second reaction above is not necessarily all liberated directly into the water or solution. Some of it may be liberated beneath the film as shown in Figure 26. The result may be local rupturing of the oxide film--a form of degradation--the formation of metal hydride, or the entry of hydrogen into the metal, depending on which are feasible or most favorable. I believe there are a number of cases where film rupture occurs, although they are often not easy to identify. We have declared the belief that it is important in the corrosion of aluminum alloys below the boiling point of water (19). To provide evidence of this, we ran a series of experiments to determine the logarithmic corrosion rate constant for 1100 aluminum at 70°C with potentials controlled by a special interrupting potentiostat (20). The results, in Figure 27, show that anodic polarization (diamond-shaped points) caused lower corrosion rates than the unpolarized runs (circular points). A reduction in cathodic damage to the film is suggested. The potential above which hydrogen should not be liberated cannot be identified because the local pH during anodic polarization could be considerably below the 6+ of the distilled water at 70°. We shall see something enlightening on this later. For pH 6 the potential for the reversible hydrogen liberation reaction is calculated to be about -0.4 volt.

Most notably at higher temperatures, aluminum also suffers from the entry of corrosion product into the

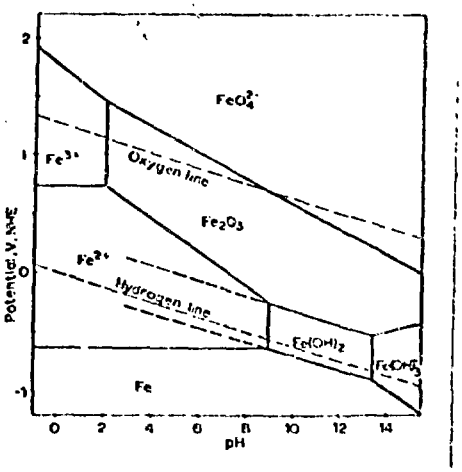

Figure 25. Pourbaix diagram for the system Fe-H_2O at 25°C (17). Reprinted courtesy Marcel Dekker, Inc.

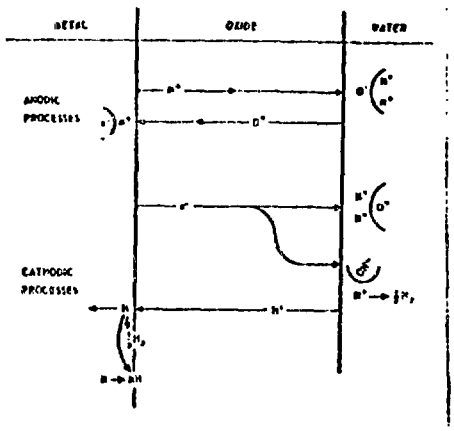

Figure 26. Schematic representation of corrosion processes (18). Reprinted courtesy Electrochem. Soc.

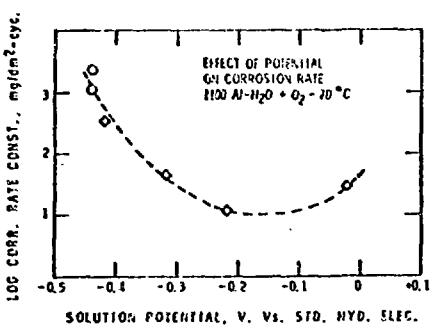

Figure 27. Effect of controlled solution potential on logarithmic corrosion rate constant for aluminum (12).

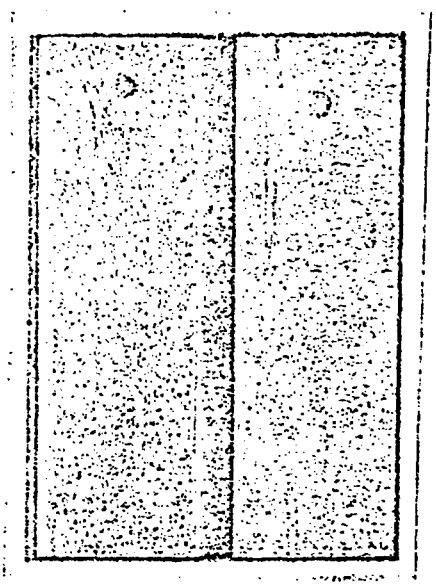

Figure 28. Typical appearance of 1100 Al after about two weeks in distilled water at 275°C (18). Reprinted courtesy Electrochem. Soc.

metal. In Figure 28 are shown specimens of commercially pure aluminum after two weeks exposure to water at 275°C. The blistering progresses with more severe exposure conditions, as shown in Figure 29 (66 hours, 300°C). Some of the blisters are hollow before the water gains access and before they become oxide-metal mixtures. Figure 30 shows what happens at a higher temperature; this exposure was four hours at 315°C. If varying amounts of material are etched from the surface of a series of samples corroded for a brief period, and each remaining sample is analyzed for hydrogen content, the hydrogen in the etched-off layers can be calculated. The results in Figure 31 show that the hydrogen content of the surface layers increased quite a bit, and demonstrate that the gas that formed the blisters was hydrogen. If the hydrogen is produced largely at a position remote from the metal surface, as in Figure 32, the severe damage is prevented. In this case, the aluminum is simply bolted to a piece of stainless steel. Exposure conditions were as in Figure 30. If to the water are added ions that are reducible to metal (largely at active cathode spots) metal dendrites are formed. The nickel dendrites in Figure 33 were formed in this way; no severe corrosion of 1100 aluminum was observed during corrosion exposure to stable nickel salt solutions at elevated temperatures. Figure 34 suggests that if deposits of something like the nickel-aluminum compound $NiAl_3$ were used they would act as very effective cathodes for hydrogen liberation. For this reason, we made aluminum-nickel alloys in which $NiAl_3$ precipated. As indicated in Figure 35, some 1% nickel alloys showed excellent corrosion resistance in high temperature water. I won't discuss details of composition and metallurgical preparation; they were found to be important.

Uranium corrodes in oxygen-free water at a constant rate to form UO_2 in the form of a relatively unprotective layer; Figure 36 shows such corrosion rates on an Arrhenius plot. When the rate gets very large at elevated temperatures, uranium hydride can be found mixed in with the oxide powder. If oxygen is present in the water, for a long period protective oxide films are formed; these eventually break down locally and spread. Figure 37 shows that the whole surface eventually becomes bad. We believe that some hydride was regularly formed beneath the oxide both in deaerated and aerated water, and that the hydride subsequently was converted to the more stable oxide. This is believed to be a case of film degradation by the formation of hydride beneath it. For selected uranium alloys, oxide films

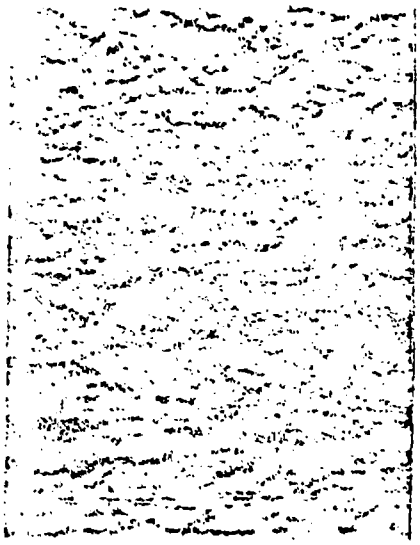

Figure 29. Surface of "normal" 1100 aluminum sample after 66 hours in distilled water at 300°C 20X (21). Reprinted courtesy Nat'l. Assoc. Corrosion Engineers.

Figure 30. 1100 aluminun after four hours in distilled water at 315°C (22). Reprinted courtesy Nat'l. Assoc. Corrosion Engineers.

TREATMENT	AVERAGE METAL ETCHED AWAY	HYDROGEN CONTENT (WHOLE SAMPLE)	ESTIMATE OF HYDROGEN IN INCREMENTS OF ETCHED METAL
AS CORRODED	-	12.1 ppm	-
AS STRIPPED	-	7.3	
ETCHED (DILUTE HNO_3-HF)	0.016 mm	3.0	280 ppm
ETCHED "	0.041	1.8	59
ETCHED "	0.071	1.1	24
ETCHED "	0.120	1.0	5
ETCHED "	0.22	0.8	3
BLANK (NO CORROSION)	-	0.6	-

Figure 31. Hydrogen analyses of 1100 aluminum after 2 days corrosion in water at 290°C (23).

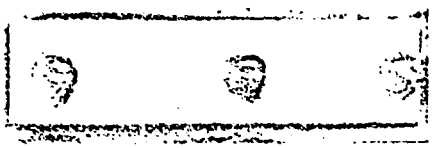

Figure 32. 1100 aluminum, coupled to 347 stainless steel, after four hours in distilled water at 315°C (22). Reprinted courtesy Nat'l. Assoc. Corrosion Engineers.

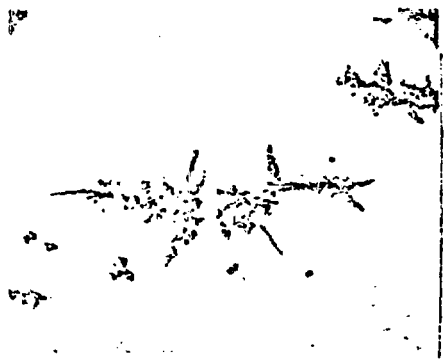

Figure 33. Dendritic nickel deposited on 1100 aluminum from $NiSO_4$ solution (50 ppm Ni^{++}) 250 X (21). Reprinted courtesy Nat'l. Assoc. Corrosion Eng'rs.

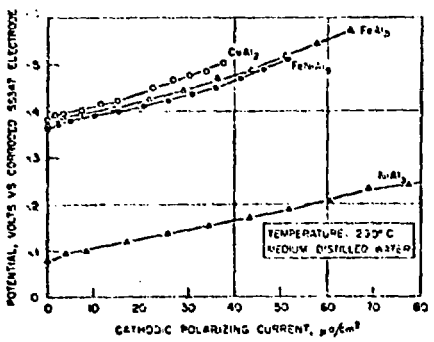

Figure 34. Cathodic polarization curves for some aluminum intermetallic compounds (9).

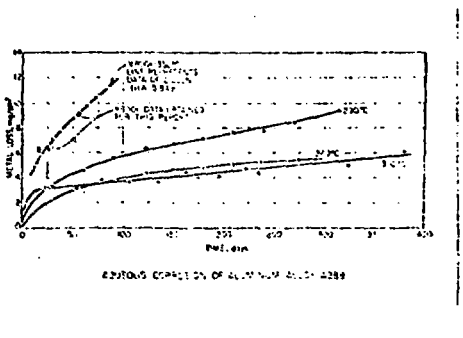

Figure 35. Aqueous corrosion of aluminum alloy A288 (Al + 1% Ni), 0.5% Fe, 0.1% Ti) (24).

are protective even in the absence of oxygen, and for very long periods. Figure 38 shows some corrosion rates which are respectably low. The maximum temperature shown is 400°C. These films also break down eventually, and this appears to involve the formation of some uranium hydride locally. The breakdown certainly involves the buildup of hydrogen in the metal. For the particular alloy and temperature in Figure 39 specimens lasted much longer before damage occurred when they were pretreated in a vacuum before corroding.

When zirconium is oxidized in water, a considerable fraction of the corrosion product hydrogen enters the metal. There is evidence that the oxide recrystallization and the transition in kinetics that were shown in Figure 19 are related to a buildup of hydrogen in the surface of the metal. It has been suggested that at that time some zirconium hydride forms beneath the film. The addition of alloying elements which form active cathodes for hydrogen liberation have reduced hydrogen uptake, have delayed transition, and have resulted in the formation of more coherent oxide after transition. There has been no clear resolution as to mechanisms (29).

It is possible to consider gaseous oxidation producing a stable oxide film as an electrochemical process in which oxidation occurs at the metal-oxide interface where metal ions leave the metal (see Figure 4) and reduction occurs at the outer surface of the oxide where electrons combine with oxygen. On the basis of this line of reasoning it is possible to predict (a) the formation of a potential difference between metal and oxide exterior for those systems in which the resistance or "retardance" to the passage of ions through the growing oxide is not much greater than the retardance to the passage of electrons, and (b) a change in oxidation rate from the application of an electrical potential between metal and oxide exterior. An illustration is the behavior of zirconium for which a potential in excess of one volt can be measured (Figure 40) and whose oxidation rate at points of electrical contact can be markedly influenced (Figure 41). The contact consisted of points at which the specimen rested upon conducting powder. Since the area of contact diminished under sharpening points of anodically stimulated growth and increased where growth was retarded cathodically, the rate of weight gain for the entire specimen in the figure was considerably more reduced by applied cathodic current than it was accelerated by applied anodic current.

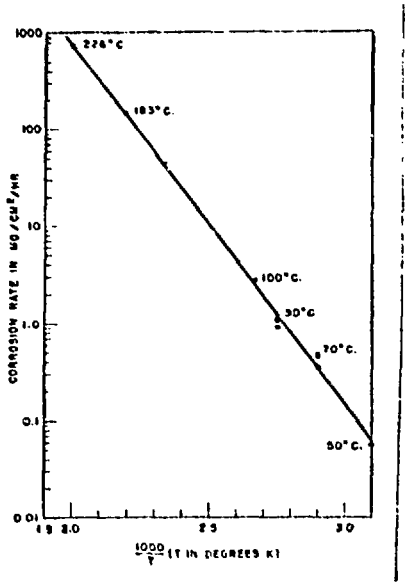

Figure 36. Corrosion rate of uranium in hydrogen-saturated water (25).

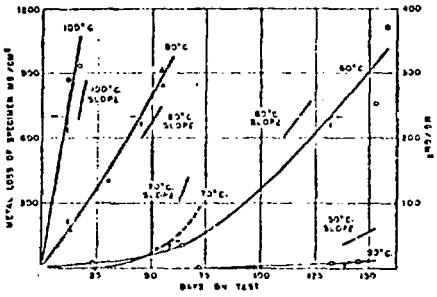

Figure 37. Corrosion of uranium in aerated distilled water (26).

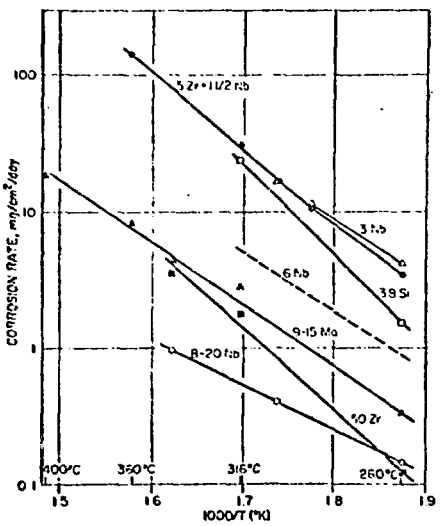

Figure 38. Corrosion of uranium alloys in water (27).

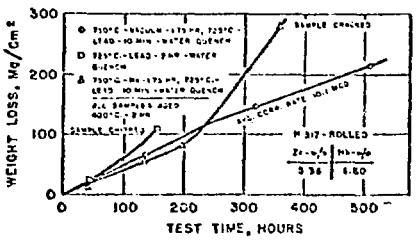

Figure 39. Effect of gas removal on corrosion in water at 290°C of U-5% Zr-1½% Nb alloy (28). Reprinted courtesy Electrochem. Soc.

Before we finish, I'd like to spend a few minutes on pitting. As you know, there are local sites at which corrosive attack occurs for some systems preferentially. If this local attack continues, quite deep pits can form. This is one of the insidious kinds of corrosion attack for a material. Some of the film-forming metals tend to be quite susceptible to pitting attack under appropriate conditions. One of the characteristic requirements for it is the formation of low pH within a protected pit--protected in some way from the general environment. We think that commonly there are local cathodes at which hydrogen liberation is very great, at which film rupture occurs. This is made easier by the fact that the cathodes are often a second, cathodic phase so there is often an imperfection in the oxide at the point anyhow. At first there is a high anodic reaction rate next to the cathode because of the proximity. When the anodic reaction has undercut the cathodic particle destroying electrical contact, the two half-cell reactions will no longer be very close together and there will be pH changes so that the anode area will become acid. The result of this is that a protective film doesn't form as a primary product of the reaction; instead, metal ions are formed in solution. As these ions diffuse out to the surface of the oxide film, the environment becomes more nearly neutral and oxides precipitate. This leads to the characteristic barnacled appearance of a pit, with precipitated oxide over it. In this way the solution within the pit is isolated from the bulk solution, and the acidity can be great. If the barnacle becomes a sufficiently effective barrier to the flow of the ionic current which must pass through the solution from remote cathodes, the pit stops growing. Figure 42 shows the cleaned surface of a ground piece of 1100 aluminum after about 4 hours in oxygen-saturated distilled water. There are occasional small pits (black in the photograph). After nearly two years exposure (Figure 43), there are no large pits; the appearance is as if essentially all of the surface had in turn served as the location for micro pit formation. The low conductivity of the water might have contributed to early stifling of pit growth. At higher magnification the pits (Figure 44) are not unlike larger ones seen in other systems. Presumably another lecturer in this series will give or has given you some details of practical pitting problems and the most promising approaches to control them.

A number of investigators have made efforts to measure the pH in pits; values as low as 1.5 have

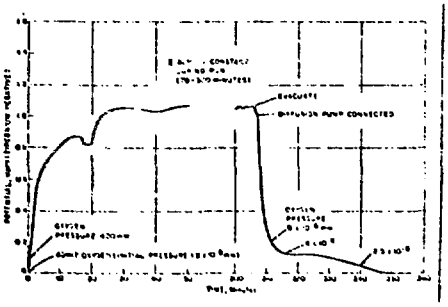

Figure 40. Potential developed during oxidation of zirconium at 700°C (30). Reprinted courtesy Electrochem. Soc.

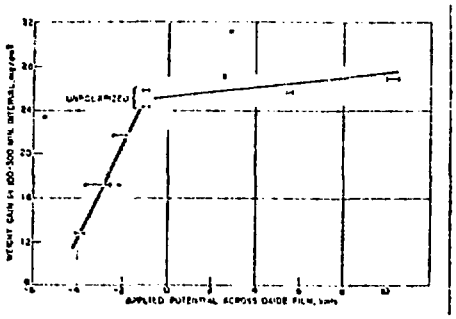

Figure 41. Variation in oxidation rate with applied potential: zirconium in oxygen at 700°C (30). Reprinted courtesy Electrochem. Soc.

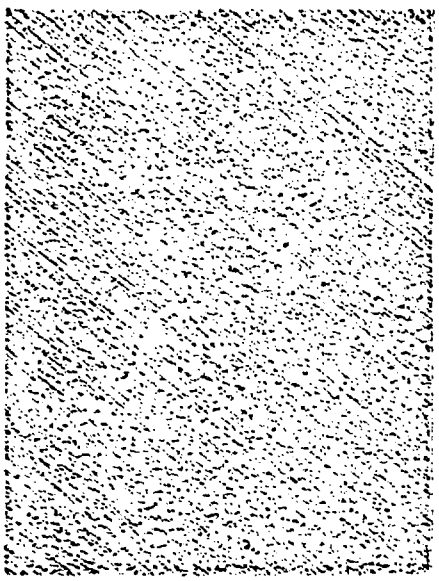

Figure 42. Cleaned 1100 aluminum surface after 4½ hours in O_2-saturated distilled water at 70°C 25 X (11).

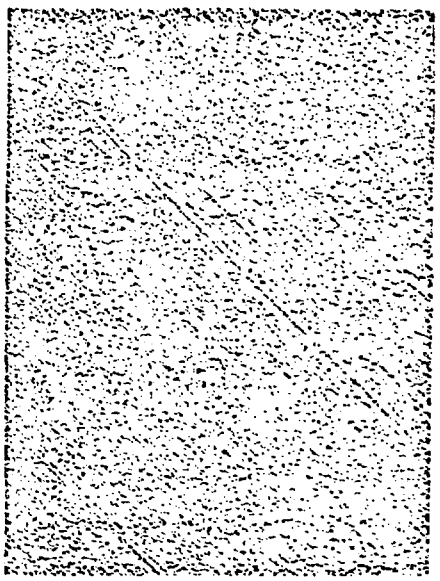

Figure 43. Cleaned 1100 aluminum surface after 704 days corrosion in O_2-saturated distilled water at 70°C 25X (11).

been reported. Even exposed to the bulk water, we found, through the use of a special electrode a few tenths of a millimeter in tip diameter (Figure 45), that the pH near specimens of 1100 aluminum corroding in distilled water reached values below 3 (Figure 46).

Some years ago, Howard Francis, then of the Armour Research Foundation, made some time-lapse motion pictures of a potential map of the solution next to steel and aluminum alloys pitting in salt water. The presence of some active cathode points and growing pits was readily displayed. I suggested that he run the film backwards to see whether the active pits had been active cathodes just before their initiation. He later told me he had done so, and they had been with few or no exceptions.

At high temperatures film breakdown and pitting for aluminum alloys takes an unusual form especially when there is a high rate of flow of water past the metal surface. If there are a lot of specimens in the system, the corrosion rate is lower than if the area is small. The results of some exploratory experiments are shown in Figure 47. A large area (factor of 20) of aluminum alloy inhibited corrosion while a large area of stainless steel did not. The effect is certainly related to corrosion product in the system somehow. In Figure 48 one can see that the corrosion product lost from the specimen was substantially in excess of that which dissolved in the system. We thought that, at local pits and breaks the corrosion product, as it reached the oxide surface and was approximately neutralized, was swept away as particles of oxide. We thought that the addition of colloidal particles to the solution would tend to "plug" openings, reduce the loss of oxide, and lower the corrosion rate. Figure 49 shows that when a hydrated colloid was injected in to the system, a very low corrosion rate was obtained. In the same system the effects of polarizing current on corrosion rate (Figure 50) are similar to what I showed you at low temperature in Figure 27: anodic protection and cathodic stimulation.

The message I'd like to leave with you tonight is that some films are very good and very protective, some films have breaks in them, and they are moderately good, some become bad by some of the strangest mechanisms: an understanding or corrosion phenomena sometimes requires quite a bit of ingenuity.

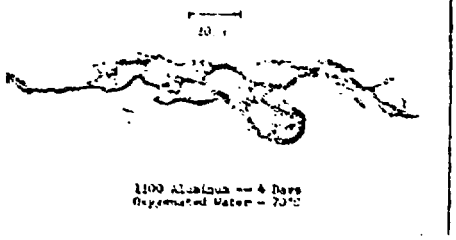

Figure 44. Electron micrograph of corroded surface of "commercially pure" aluminum (12).

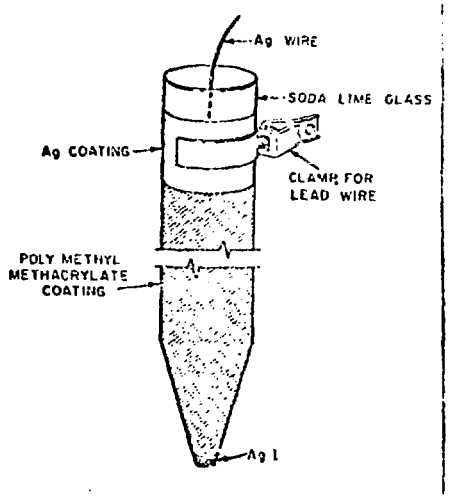

Figure 45. Glass, silver/silver iodide pH microelectrode (31). Reprinted courtesy Nat'l. Assoc. Corrosion Eng'rs.

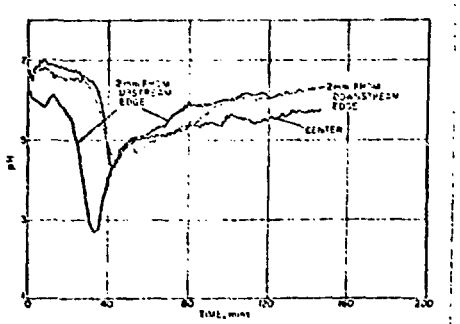

Figure 46. Effect of position on pH of 50°C oxygen-saturated water 0.1 mm from corroding 1100 aluminum (31). Reprinted courtesy Nat'l. Assoc. Corrosion Eng'rs.

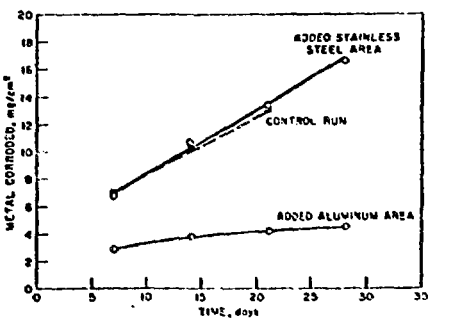

Figure 47. Effect on aqueous corrosion of 8001 aluminum at 260°C (7 m/sec vel.) of added surface of aluminum or stainless steel (32).

	Normal (small) Area, 21-day Exposure	Large Area, 28-day Exposure
Average Metal Loss	13.1 mg/cm^2	4.60 mg/cm^2
Estimated $Al_2O_3 \cdot H_2O$ Produced (from metal loss)	29.1 mg/cm^2	10.2 mg/cm^2
Actual Average Product Remaining	11.6 mg/cm^2	7.9 mg/cm^2
Corrosion Product Lost	17.5 mg/cm^2	2.3 mg/cm^2
Corrosion Product Present at End of Test Compared with Total Produced	40%	78%
Aluminum Area	70 cm^2	1470 cm^2
Maximum Dissolved Corrosion Product, from Solubility Data (2×10^{-4} g of Al_2O_3 per liter at 1.5-liters/hr refreshment)	2.4 mg/cm^2	0.14 mg/cm^2
Ratio Dissolved to Actual Loss	0.14	0.06
Corrosion Rate in Last 7-day Period	40 mdd	5.8 mdd

Figure 48. Comparison of Two Dynamic Corrosion Tests. Water at 260°C, 7 m/sec vel. (32).

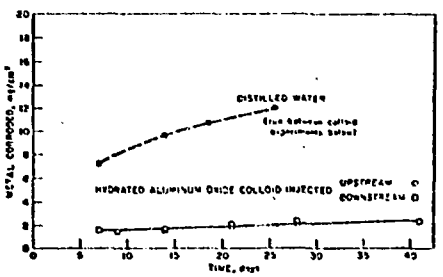

Figure 49. Influence of 35-ppm colloid on the aqueous corrosion of 8001 aluminum at 260°C, 7-m/sec velocity (32).

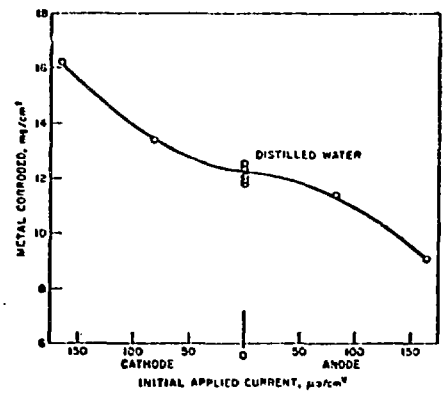

Figure 50. Effects of applied Current on corrosion of 8001 aluminum at 260°C in flowing water (5.6-m/sec) (32).

Literature Cited

1. Vijh, A. K., J. Electrochem. Soc. (1972) 116, 972.
2. Tajima, S., Baba, N., and Shimura, F. M., Electrochimica Acta (1967) 12, 955.
3. Hauffe, Karl, "Oxidation of Metals," p. 419, Plenum Press, New York, New York, 1965.
4. Hart, R. K., "Morphology of Corundum Films on Aluminum," Fifth Int. Cong. for Electron Microscopy, Philadelphia, Pennsylvania, Aug. 29 - Sept. 5, 1962, Paper No. C-10, Academic Press, New York, New York, 1962.
5. Hart, R. K., and Maurin, J. K., "Growth of Oxide Nuclei on Iron," Sixth Int. Cong. for Electron Microscopy, Kyoto, Japan, Aug. 28 - Sept. 4, 1966, p. 539, Maruzen Co., Ltd., Tokyo, Japan, 1966.
6. Ruther, W. E., and Hart, R. K., Corrosion (1963) 19, 127t.
7. Frankenthal, R. P., and Malm, D. L., J. Electrochem. Soc. (1976) 123, 186.
8. Ruther, W. E., Schleuter, R. R., Lee, R. H., and Hart, R. K., Corrosion (1966) 22, 147.
9. Ruther, W. E., and Draley, J. E., unpublished work.
10. Draley, J. E., Ruther, W. E., and Greenberg, S., J. Nucl. Matl. (1962) 6, 157.
11. Draley, J. E., TID-7587, "Aqueous Corrosion of 1100 Aluminum and of Aluminum-Nickel Alloys," Int. Conf. on Aqueous Corrosion of Reactor Mat'ls., Brussels, Oct. 14-17, 1959, p. 165, U. S. Atomic Energy Commission and European Atomic Energy Society, July 1960.
12. Draley, J. E., Mori, S., and Loess, R., unpublished figure.
13. Mori, S., and Draley, J. E., J. Electrochem. Soc. (1967) 114, 352.
14. WAPD-MRP-107, "Pressurized Water Reactor (PWR) Project Technical Progress Report October 24, 1963-January 23, 1964," Westinghouse Atomic Power Div.
15. Griggs, B., Maffei, H. P., and Shannon, D. W., HW-67818, "Multiple Rate Transitions in the Aqueous Corrosion of Zircaloy," Hanford Laboratories, General Electric Company, December 20, 1960.
16. Draley, J. E., unpublished work.
17. Diggle, John W. (Ed.), "Oxides and Oxide Films," Vol. 1, p. 38, Marcel Dekker, Inc., New York, New York, 1972.
18. Draley, J. E., and Ruther, W. E., J. Electrochem. Soc. (1957) 104, 329.
19. Draley, J. E., and Mori, Shiro, and Loess, R. E., J. Electrochem. Soc. (1963) 110, 622.

20. Youngdahl, C. A., and Loess, R. E., J. Electrochem. Soc. (1967) 114, 489.
21. Draley, J. E., and Ruther, W. E., Corrosion (1956) 12, 480t.
22. Draley, J. E., and Ruther, W. E., Corrosion (1956) 12, 441t.
23. Draley, J. E., and Ruther, W. E., ANL-5658 "Experiments in Corrosion Mechanism: Aluminum at High Temperatures," Argonne National Laboratory, April 1957.
24. Draley, J. E., and Ruther, W. E., "The Corrosion of Aluminum Alloys in High Temperature Water," IAEA Conf. Corrosion of Reactor Materials, Salzburg, June 1962, Vol. I, p. 477.
25. McWhirter, J. W., and Draley, J. E., ANL-4862 "Aqueous Corrosion of Uranium and Alloys: Survey of Project Literature," Argonne National Laboratory, May 14, 1952.
26. Mollison, W. A., English, G. C., and Nelson, F., CT-3055 "Corrosion of Tuballoy in Distilled Water," Argonne National Laboratory, June 23, 1945.
27. Greenberg, S., and Draley, J. E., unpublished figures.
28. Draley, J. E., Greenberg, S., and Ruther, W. E., J. Electrochem. Soc. (1960) 107, 732.
29. Parfenov, B. G., Gerasimov, V. V., and Venediktova, G. I., "Corrosion of Zirconium and Zirconium Alloys," Translated from Russian by Ch. Nisenbaum, Israel Program for Scientific Translations, Jerusalem, 1969.
30. Bradhurst, D. H., Draley, J. E., and Van Drunen, C. J., J. Electrochem. Soc. (1965) 112, 1171.
31. Mori, S. Loess, R. E., and Draley, J. E., Corrosion (1963) 19, 165t.
32. Draley, J. E., and Ruther, W. E., ANL-7227, "Corrosion of Aluminum Alloys by Flowing High Temperature Water," Argonne National Laboratory, January 1967.

Acknowledgement

This paper was prepared with the support of the U. S. Energy Research and Development Administration.